Biochemistry and Biophysics Reports 34 (2023) 101486

Contents lists available at ScienceDirect

Biochemistry and Biophysics Reports

journal homepage: www.elsevier.com/locate/bbrep

Comparison of mesenchymal stem cells from bone marrow, umbilical cord blood, and umbilical cord tissue in regeneration of a full-thickness tendon defect *in vitro* and *in vivo*

Ji-Hye Yea [a], Yeasol Kim [b,c], Chris H. Jo [b,c,*]

[a] Department of Pathology, Johns Hopkins University, Baltimore, MD, USA
[b] Department of Translational Medicine, Seoul National University College of Medicine, Seoul, South Korea
[c] Department of Orthopedic Surgery, SMG-SNU Boramae Medical Center, Seoul National University College of Medicine, Seoul, South Korea

ARTICLE INFO

Keywords:
Shoulder pain
Tendon regeneration
Mesenchymal stem cells
Bone marrow
Umbilical cord

ABSTRACT

Although mesenchymal stem cells (MSCs) can be obtained from various tissues such as bone marrow (BM), umbilical cord blood (UCB) and umbilical cord tissue (UC), the comparative efficacy of each MSC in tendon regeneration is unknown. Therefore, we investigated the efficacy of MSCs isolated from three different sources on tendon regeneration after injury.

We evaluated the potential of BM-, UCB- and UC-MSC to differentiate into tendon-like cells in tensioned three-dimensional construct (T-3D) using gene and histological analysis. In animal experiments, full-thickness tendon defect (FTD) was created in supraspinatus of rats, and injected with Saline and BM-, UCB- and UC-MSC. After two and four weeks, histological evaluations were performed.

After inducing tenogenic differentiation, the gene expression of scleraxis, mohawk, type I collagen and tenascin-C was upregulated by 3.12-, 5.92-, 6.01- and 1.61-fold respectively and formation of tendon-like matrix was increased 4.22-fold in UC-MSC compared to BM-MSC in T-3D. In animal experiments, the total degeneration score was lower in the UC-MSC group than in BM-MSC group at both weeks. In heterotopic matrix formation, glycosaminoglycan-rich area was reduced in the UC-MSC group, whereas area was larger in the BM-MSC group than in Saline group at four weeks.

In conclusion, **UC-MSC is superior to other MSCs in differentiating into tendon-like lineage cells** and **forming a well-organized tendon-like matrix under T-3D conditions**. **UC-MSC enhances regeneration of FTD in terms of histological properties** compared to BM- and UCB-MSC.

1. Introduction

Rotator cuff disease typically progresses irreversibly following an injury due to low healing potential of tendon [1]. Although conservative treatments have been administered to patients diagnosed with rotator cuff disease, persistent symptoms have been observed in 45% of patients after 12 months [2]. These persistent symptoms are associated with the typically avascular and acellular structure of tendon, and tenocytes which no longer participate in regeneration of tendon structure after disease [1]. Thus, new biological strategies are needed for regeneration of tendon structure [3,4].

Since the discovery of adult bone marrow (BM)-derived mesenchymal stem cells (MSCs) in 1976 by Friedenstein et al., BM-MSC have been studied and used in fundamental tissue regeneration [5–7]. Although the use of BM-MSC is suggested as the 'golden standard' in tissue engineering field, the therapeutic application of BM-MSC is limited by invasive harvesting techniques [8], poor collection efficiency [9], deterioration in quality with age and donor morbidities [10], and the risk of heterotopic matrix formation such as ossification [10]. Therefore, other promising MSCs are needed to overcome these drawbacks.

Recently, cells of perinatal and fetal origin have been mentioned as alternate sources for MSCs. Umbilical cords, which are commonly discarded as medical waste after delivery, can be obtained non-invasively and at a relatively low cost [9]. In a rabbit model of full-thickness rotator cuff injury, umbilical cord blood (UCB)-derived MSCs fill the

* Corresponding author. Department of Orthopedic Surgery, SMG-SNU Boramae Medical Center, Seoul National University College of Medicine, 20 Boramae-ro 5-gil, Dongjak-gu, Seoul, 07061, South Korea.
E-mail address: chrisjo@snu.ac.kr (C.H. Jo).

https://doi.org/10.1016/j.bbrep.2023.101486
Received 14 February 2023; Received in revised form 15 April 2023; Accepted 11 May 2023

defective tendon by forming a tendon-like matrix and induce functional recovery [11]. However, the number of MSCs in UCB is remarkably low, and it is difficult to obtain MSCs from UCB similar to BM [12]. MSCs isolated from umbilical cord tissue (UC), on the other hand, exhibit rapid growth and higher self-renewal capacity than other MSCs [12,13]. UC-MSC have been shown to regenerate tendon matrix and improve tensile strength of rotator cuff tendon in a rat model of full-thickness rotator cuff tendon defect [14]. Although previous studies suggested that MSCs isolated from fetal sources may be better therapeutic candidates than BM-MSC in immune-related disease [6,15], the comparative efficacy of MSCs isolated from different sources such as BM, UCB and UC on tenogenic differentiation and tendon regeneration of rotator cuff has yet to be reported.

Therefore, this study aimed to compare three different sources of MSCs based on tenogenic differentiation and tendon matrix formation under tensioned three-dimensional constructs (T-3D) as well as tendon regeneration in a rat model of full-thickness tendon defect (FTD).

2. Materials and methods

2.1. Isolation and culture of BM-, UCB- and UC-MSC

This study was approved by the Seoul Metropolitan Government Seoul National University Boramae Medical Center Institutional Review Board (IRB No. 16-2015-115). Informed consent was obtained from all patients before performing the study. Detail information of donors was shown in Supplementary Table 2.

Extracted BM was diluted with Dulbecco's Phosphate-Buffered Saline (DPBS; Welgene, Daegu, Korea) and layered on top of Ficoll-Paque Premium (GE Healthcare, Uppsala, Sweden) at a ratio of 1:2, followed by centrifugation at 400*g* (with the brake off) for 30 min at 20 °C. The uppermost layer was aspirated and discarded. The mononuclear layer was then collected and diluted with DPBS at a ratio of 1:2. This suspension was centrifuged at 400 g for 5 min and washed again with DPBS. The supernatant was discarded and the pellet was resuspended with 10 mL growth medium; low-glucose Dulbecco's modified Eagle medium (LG-DMEM; Hyclone, Logan, USA) supplemented with 10% fetal bovine serum (FBS; Hyclone) and antibiotic-antimycotic solution (100 U/mL penicillin, 100 μg/mL streptomycin, and 0.25 μg/mL amphotericin B; Welgene). The suspension was centrifuged at 400 g for 5 min. The cellular pellet was resuspended in growth medium. Cells (3×10^3 cells/cm^2) were plated onto conventional tissue culture plates.

UCB MSCs were purchased from Cyagen Biotechnology Inc. (HUXUB_01001, Cyagen, Biosciences, Santa Clara, CA, USA) and cultured according to the recommended protocol of Cyagen. Cyagen has certified that the UCB MSCs have ability to multipotent differentiation along the osteogenic, chondrogenic, and adipogenic lineages. Moreover, the cells are positive for CD29, CD44, CD73, CD105, and CD166, and negative for CD11a, CD34, and CD45 according flow cytometry results.

Human umbilical cord tissues were collected from term infants delivered via cesarean section. Isolated umbilical cord tissues were washed 2 to 3 times with DPBS to remove blood products, followed by sectioning into minimal cube explants of 2–4 mm each, using surgical scissors. The cube explants (1 g) were aligned at regular intervals in 15-cm culture dishes and allowed to firmly attach to the bottom of the dish for 60 min in a 5% CO_2 incubator with humidified air at 37 °C. The growth medium was gently poured into the dishes. The medium was replaced twice a week. Non-adherent cells were removed by changing the medium. When cells reached 80% confluency, they were detached by trypsin-ethylendiaminetetracetic acid (EDTA) (0.05% trypsin, 0.53 mM EDTA; Welgene). The tissues were removed by passing through a 100 μm cell strainer (SPL Life Sciences, Pocheon, Korea). The cells were centrifuged at 500 g for 5 min at 20 °C, and then replated at a density of 3×10^3 cells/cm^2.

MSCs were incubated in a 5% CO2 incubator with humidified air at 37 °C and the medium was replaced every 3 days. At 70–80% confluence, the cells were split at a ratio of 1:3. BM and UCB MSCs were used at passage 5, and UC MSCs were used at passage 10 for *in vitro* and *in vivo* experiments.

2.2. Characterization of BM-, UCB- and UC-MSC

When BM-, UCB- and UC-MSC reached 70–80% confluence, cell morphologies were observed under a light microscopy. Cell viability of MSCs was determined by trypan blue exclusion and live and dead cells were counted using hemocytometer. The percentages of cell viability of MSCs were calculated using the following formula: total number of live cells/total number of cells x 100 (%) [14].

Cell preparation for flow cytometry was conducted according to previously described methods with modification [16]. Briefly, total of 7 antibodies were used in flow cytometry: CD11a-FITC, CD34-FITC, CD45-PE, CD73-FITC, CD73-PE, CD90-FITC, and CD105-FITC (BD Biosciences, San Jose, CA, USA). 5×10^5 cells were aliquoted in each tube, stained with antibodies for 30 min at 4 °C in the dark room. Data were obtained by analyzing 10,000 events on a FC500 Flow Cytometer (Beckman Coulter, Brea, CA, USA).

BM-MSCs and UC-MSCs were subjected to *in vitro* multi-lineage differentiation using the previously described formulas with modification [17]. Briefly, for the adipogenic differentiation, MSCs were seeded into the 24-well plate at 0.75×10^4 cells/cm^2 and induced with dexamethasone (1 μM), indomethacin (60 μM), 3-isobutyl-1-methylxanthine (500 μM), and insulin (5 μg/mL) (all reagents from Sigma-Aldrich). Oil Red O staining assay was conducted after 21 days. For the osteogenic differentiation, MSCs were seeded at the same density and induced with dexamethasone (0.1 μM), L-ascorbic acid 2-phosphate sesquimagnesium salt hydrate (50 μg/mL), and β-glycerophosphate disodium salt hydrate (10 mM) (all reagents from Sigma-Aldrich). Von Kossa staining assay was conducted after 21 days. MSCs were seeded at 2×10^5 cells/5 μL in a 15-mL polypropylene tube for the chondrogenic differentiation and induced with dexamethasone (0.1 μM), L-ascorbic acid 2-phosphate sesquimagnesium salt hydrate (50 μg/mL), 1X insulin-transfer-selenium-X (Gibco, Waltham, MA, USA) L-proline (40 μg/mL), sodium pyruvate (100 μg/mL), and TGFβ-1 (10 ng/mL) (PeproTech, Rocky Hill, NJ, USA). Alcian Blue staining assay was conducted after 21 days (Sigma-Aldrich).

2.3. Tensioned three-dimensional construct (T-3D) for tenogenic differentiation of MSCs

A 5 mL aliquot of Sylgard (Dow Corning, Midland, MI, USA) was added to 6-well plates. Two cotton thread sutures approximately 5 mm in length were pinned to the Sylgard surface of dishes, 15 mm apart, using stainless steel minutien pins (Interfocus, Cambridge, UK). The dishes were sterilized by soaking in 70% ethanol for 1 h and then washed with DPBS twice. After air drying, growth medium was added for 24 h. After removing pre-soaking media, MSCs (5×10^5 cells/well) in 1 mL growth medium supplemented with 2 mg fibrinogen (F3879 Sigma-Aldrich), 1 μL aminohexanoic acid (07260 Sigma-Aldrich), and 1 μL aprotinin (10236624001 Roche, UK) were mixed with 0.5 U thrombin (Reyon Pharmaceutical, Weoul, Korea) per well. The MSCs were then layered on culture dish, followed by incubation for 3 h at 37 °C, and addition of 3 mL growth medium supplemented with ascorbic acid 2-phosphate (250 μM; Sigma-Aldrich) and proline (50 μM; Sigma-Aldrich). Culture plates were incubated at 37 °C and 5% CO2 for the duration of the experiment. Media were changed every 3 days. The samples were harvested on days 0, 3, 7 and 14 for gene evaluation (n = 4), and on days 7 and 14 for histological evaluation (n = 4) [18].

2.4. RNA isolation and quantitative real-time reverse transcriptase polymerase chain reaction (qRT-PCR)

Total RNA was extracted, and reverse transcription and

amplification were performed as previously describe [19]. Briefly, the total RNA was extracted using RNeasy® mini kit (QIAGEN, Hilden, Germany) and quantified using a NanoDrop ND-100 spectrophotometer (NanoDrop, Wilmington, Delaware). First-strand complementary DNA (cDNA) was synthesized with 1 μg of mRNAs using Superscript III Reverse Transcription kit (Invitrogen, Carlsbad, CA). The synthesized cDNA was diluted to 300 μl with PCR-grade water and then stored at −20 °C until use.

To perform real-time PCR utilizing a LightCycler480 (Roche Applied Science, Mannhein, Germany), TaqMan® Gene Expression Assays (Applied Biosystems, Foster City, CA) were used with genes related to tenogenic differentiation such as scleraxis (SCX) and mohawk (MKX); tendon matrix such as type I collagen (COL1), tenascin-C (TNC); adipogenic differentiation such as peroxisome proliferator-activated receptor γ 1 (PPARγ1); chondrogenic differentiation such as SRY-Box Transcription Factor 9 (SOX9); and osteogenic differentiation such as runt-related transcription factor 2 (RUNX2). The information about the probes was provided in S. Table 1. The PCRs were performed in a final volume of 20 μl containing 10 μl 2xLightCycler® 480 Probes Master (Roche Applied Science), 1 μl TaqMan® Gene Expression Assay (Applied Biosystems), 5 μl cDNA as the template, and 4 μl PCR-grade water under the following conditions: 95 °C for 10 min, 40 cycles of 95 °C for 10 s and 60 °C for 1 min, followed by 72 °C for 4 s, and a final cooling step at 40 °C for 30 s. Gene expressions were normalized versus GAPDH0 by normalizing the cycle number at which each gene transcript was detectable (threshold cycle, Ct) against Ct of GAPDH, which is referred to as ΔCt. Gene expressions relative to GAPDH are expressed as $2^{-\Delta Ct}$, where $\Delta Ct = Ct_{\text{gene of interest}} — Ct_{GAPDH}$. All experiments were performed in triplicate and the average values were calculated for normalized levels of expression using its own day 0 values [19].

2.5. Matrix formation by BM-, UCB- and UC-MSC

The harvested samples were immediately fixed and embedded in paraffin blocks. The tissue was carefully trimmed to appropriate middle site of sample and cut into 4-μm-thick serial sections.

Slide were stained with hematoxylin and eosin (H&E) for general appearance, picrosirius red (PSR) for analysis of collagen fiber organization and coherency. Collagen organization was measured as intense white areas of brightly diffracted light on gray scale (black, 0; white, 255) using ImageJ software with installed NII plugin (National Institutes of Health, MD, USA). Higher value indicates more organized and mature collagen fibers [27]. The value of coherence is a measure of the extent of fiber alignment in the major axis of alignment. The coherence was quantified using the Orientation J plug-in for ImageJ and then multiplied by 100 to obtain the final coherence value. Higher value indicates more parallel collagen fibers. Five ROIs were measured, and the mean value was used. Further, the slides were stained immunohistochemically (IHC) to assess type I collagen formation, using rabbit anti-type 1 collagen (1:600 dilution, Abcam; ab34710). Detailed procedures are described in a previous study [14].

2.6. In vivo study

Animal procedures were conducted in accordance with the protocol approved by the Seoul Metropolitan Government Seoul National University Boramae Medical Center Institutional Animal Care and Use Committee (IACUC_2019_0006). Thirty-two adult male Sprague-Dawley rats (12 weeks old, 340–360 g) were divided into one of four groups and treated accordingly: 1) Saline; 2) BM-MSC; 3) UCB-MSC; and 4) UC-MSC. Rats from each group were sacrificed 0, two and four weeks after surgery. The supraspinatus tendon (SST) was harvested and used for histological and cell trafficking evaluation (n = 4) [14].

Anesthesia was induced using a mixture of zoletil and rompun (30 mg/kg + 10 mg/kg). The left shoulder was operated in all cases. A 2 cm skin incision was made directly over the anterolateral border of the acromion. After the SST was exposed by detaching trapezius and deltoid muscle from the acromion, a round FTD with a diameter of 2 mm in middle of the SST was created using a Biopsy Punch. Ten microliters of saline, BM-, UCB- and UC-MSC (1×10^6 cells in saline) were intratendinously injected adjacent to the defect tendon bilaterally in two divided doses using a 30 G needle. Detailed procedures are described in a previous study [14].

2.7. Histological evaluation of FTD in rotator cuff tendon of rats

After the macroscopic evaluation, the harvested tissues were immediately fixed in 4% (w/v) PFA (Merck, Darmstadt, Germany) for 24 h, followed by decalcification in 10% EDTA (Sigma-Aldrich, St Louis, MO, USA) for two days. After decalcification, the tissues were dehydrated through an increasing series of ethanol gradient, defatted in chloroform, and embedded in paraffin blocks. The tissue was carefully trimmed to the appropriate middle site of tendon and cut into 4-μm-thick serial sections.

A randomly selected slide was stained with H&E and analyzed. The tendinopathy was evaluated by analyzing each slide using the semi-quantitative grading scale as previously described [20]. The 7 parameters of the system include fiber structure, fiber arrangement, rounding of the nuclei, variations in cellularity, vascularity, stainability, and hyalinization. Each parameter in the grading scale varies from 0 to 3; 0 indicated a normal appearance, 1 slightly abnormal, 2 moderately abnormal, and 3 markedly abnormal. The following scheme was used: fibre structure (0 = linear, no interruption, 3 = short with early truncation); fiber arrangement (0 = well ordered and regular, 3 = no pattern identified); rounding of nuclei (0 = flat, 3 = rounded); variations in cellularity (0 = uniform; 3 = high regional variation); vascularity (0 = absent, 3 = high); stainability (0 = vivid, 3 = pale); and hyalinization (0 = absent, 3 = high). The total degeneration score for a given slide varied between 0 (normal tendon) and 21 (most severe degeneration).

We also evaluated heterotopic ossification when separated, clustered and bar-shaped foci were found in whole tendon structure using H&E slides [21].

Slides were stained with PSR for analysis of collagen fiber organization and coherence using circularly polarized light microscopy. Further, the slides were stained immunohistochemically to assess type I collagen formation after injury, using rabbit anti-type 1 collagen (1:300 dilution, abcam; ab34710).

The cartilage formation was evaluated by staining slides with safranin-O/fast green and observed via light microscopy at ×40 magnification. The glycosaminoglycan (GAG)-rich area was measured using image J [14,22].

2.8. Human MSCs trafficking

Anti-human mitochondrial antibody (1:500; ab92824, Abcam, Cambridge, UK) was used to detect the injected human MSCs at two and four weeks. The antibody-positive cells were counted in each area and the mean number was used in image J. Detailed procedures are described in a previous study [23,24].

2.9. Statistical analysis

All data are expressed as the mean ± SD. The data were analyzed using two-way analysis of variance for characterization of MSCs and gene expressions and one-way analysis of variance (ANOVA) with post-hoc analysis by Bonferroni multiple comparison tests for other analysis. All statistical analyses were performed with SPSS software version 23 (IBM, Chicago, USA). Differences of $p < 0.05$ were considered statistically significant.

3. Results

3.1. Characterization of BM-, UCB- and UC-MSC

All MSCs showed fibroblast-like morphology. Viabilities of BM-, UCB- and UC-MSC were 99.00 ± 1.00%, 98.69 ± 0.58%, and 99.69 ± 0.58%, respectively, in trypan blue assay. There is no significant difference among MSC groups (Fig. 1).

To detect surface markers and characterize the BM-MSCs and UC-MSCs which we isolated from human samples, the expression levels of surface makers were measured by flow cytometry (S. Fig. 1). MSCs exhibited similar phenotypes: positive for CD73 CD90 and CD105, negative for CD11a, CD34, and CD45.

The differentiation capacity of MSCs was assessed through induction towards adipogenic, osteogenic, and chondrogenic lineages. To confirm adipogenic differentiation, the expression levels of PPARγ, LDL, and AP2 were measured (S. Fig. 2A–C), revealing a higher PPARγ expression in UC-MSCs compared to BM-MSCs by the third week. Additionally, Oil Red O assay result showed slightly higher level in BM-MSCs at the same time point (S. Fig. 2D and E). To confirm osteogenic differentiation, the gene expression levels of RUNX2, ALP, and OPN were examined (S. Fig. 3A–C), revealing the gene expression levels of BM-MSCs at all time points were greater than UC-MSCs. Von Kossa assay result confirmed higher level in BM-MSCs (S. Fig. 3D and E). To confirm chondrogenic differentiation, the gene expression levels of SOX9, Acan, and Col2 were examined (S. Fig. 4A–C), and similar to osteogenic differentiation, BM-MSCs showed higher expression levels at all time points. Safranin O assay result also confirmed higher level in BM-MSCs (S. Fig. 4D and E). These results showed that the cells have multipotent differentiation potential.

3.2. Gene expression related to tenogenic, adipogenic, chondrogenic and osteogenic differentiation

To compare the abilities of tenogenic differentiation, the cells were cultured in T-3D culture system. The MSC-seeded fibrin gel contracted around two fixed suture points and formed a longitudinal tendon-like structure over the culture period. Especially, the fibrin gel seeded with UC-MSC contracted and formed longitudinal structure only after 1 day and other gels seeded with BM- and UCB-MSC needed at least 3 days to form longitudinal structure (Fig. 1C).

Tenogenic differentiation related gene expressions including SCX and MKX was significantly upregulated in all MSCs. Gene expression of SCX was the highest in UC-MSC (7.66-fold) among MSCs groups (BM-MSC, 2.45-fold; UCB-MSC, 2.28-fold) on day 3. UCB-MSC showed a 1.61-fold higher gene expression than BM-MSC, whereas no significant difference was found between groups on day 7 (Fig. 1D). Gene expression of MKX was significantly upregulated in UC-MSC (12.94-fold) compared to BM-MSC (2.18-fold and UCB-MSC (6.66-fold) by day 14. UCB-MSC showed significantly higher gene expression of MKX than BM-MSC by 3.05-fold (Fig. 1E).

Tendon matrix-related gene expression including COL1 and TNC was significantly upregulated in all MSCs. Gene expression of COL1 was the highest in UC-MSC (7.62-fold) compared with other MSC groups (BM-MSC; 1.30-fold and UCB-MSC; 1.27-fold) on day 7. UCB-MSC showed a 1.63-fold higher gene expression than BM-MSC, while there was no significant difference between groups on day 3 (Fig. 1F). Gene expression of TNC was the highest in UC-MSC, followed by UCB-MSC, and BM-MSC, while no significant difference existed among the groups on day 7 (Fig. 1G).

Although the levels of adipogenic and chondrogenic differentiation markers such as PPARγ1 and SOX9 were slightly changed, no noticeable change in gene expression occurred in any group. However, gene expression of RUNX2 related to osteogenic differentiation was significantly upregulated in BM-MSC by 4.54-fold, whereas no significant upregulation of gene expression was detected in UCB- (1.23-fold) and UC-MSC (1.48-fold) by day 3 (Fig. 1H–J). There results showed that UC-MSC had the highest potential for tenogenic differentiation while BM-MSC had the potential for osteogenic differentiation even in the condition of induced tenogenic differentiation.

3.3. Tendon-like matrix formation in T-3D conditions

Next, cell morphology changes and tendon-like matrix formation were investigated. After 7 days, all MSC groups showed a fibroblast-like morphology. By day 14, the cells carried more flattened nuclei and aligned parallel to the gel axis in UC-MSC group compared with those in BM- and UCB-MSC (Fig. 2A).

A collagen matrix was formed in all MSC groups. Collagen organization was the highest in UC-MSC (79.1 ± 8.13 and 155.46 ± 24.08), followed by UCB-MSC (45.81 ± 19.06 and 100.74 ± 16.43), and BM-MSC (18.75 ± 2.61 and 72.21 ± 8.07) on days 7 and 14, respectively, and no significant difference existed among the different groups. The matrix formed by MSCs was composed of type I collagen (Fig. 2B–D).

Collagen fiber coherence was the highest in UC-MSC (0.78 ± 0.05), followed by UCB-MSC (0.65 ± 0.04), and BM-MSC (0.55 ± 0.05), with significant difference between the groups on day 7. After 14 days, the value was significantly higher in UC-MSC by 0.80 ± 0.09 than in BM-MSC by 0.66 ± 0.04 and UCB-MSC by 0.71 ± 0.06, respectively, whereas no significant difference was detected between BM- and UCB-MSC (Fig. 2B and E). These results demonstrated that UC-MSC exhibited a phenotype mostly like tenocytes and produced the highest amount of tendon-like matrix compared to other cell types.

3.4. Histological evaluation of FTD in rotator cuff tendon of rats

To investigate the effect of three different types of MSCs on tendon regeneration after injury. A FTD rat model was used and was administrated by three different cells. After 2 and 4 weeks, histological evaluation was performed. The total degeneration score showed no significant difference between MSC groups and Saline group in two weeks. After four weeks, the total degeneration score was significantly lower in all MSCs including BM-MSC (13.13 ± 0.99), UCB-MSC (11.25 ± 0.89) and UC-MSC (7.50 ± 0.93), respectively, than in Saline (15.50 ± 0.53). Among MSC groups, UC-MSC showed a significant recovery compared to BM-MSC and UCB-MSC. UC-MSC had lower scores than UCB-MSC. The differences between groups were based on parameters including fiber structure, variations in cellularity, and hyalinization, which were significantly lower in UC-MSC than in BM- and UCB-MSC (Fig. 3A and B).

We found no heterotopic ossification in any group at any time point (Fig. 3A).

At two weeks, the collagen organization and collagen fiber coherence were not significantly different between MSCs groups and Saline group. After four weeks, collagen organization increased in all MSCs: BM-MSC (83.30 ± 14.30), UCB-MSC (82.19 ± 8.21) and UC-MSC (103.60 ± 16.88) compared with Saline (63.36 ± 15.45), but only the score of UC-MSC was significantly higher than that of Saline. The regenerated tendon matrix in UC-MSC was composed of high-density type I collagen while Saline showed low levels of low-density type I collagen (Fig. 4A–C).

The collagen fiber coherence was significantly improved in UC-MSC (44.15 ± 4.94) compared with Saline (20.88 ± 6.80) and BM-MSC (23.61 ± 8.86). The collagen fiber coherence in UCB-MSC was also improved compared with Saline, with no significant difference between the groups (Fig. 4A and D).

In terms of GAG-rich area, the values showed no significant difference between MSC groups and Saline group at two weeks. After four weeks, the area was significantly reduced in UC-MSC (176.16 ± 63.28 mm^2) compared with Saline (939.50 ± 148.66 mm^2), whereas the area was significantly larger in BM-MSC (1428.32 ± 134.16 mm^2) than in Saline group. There was no significant difference between BM-MSC and

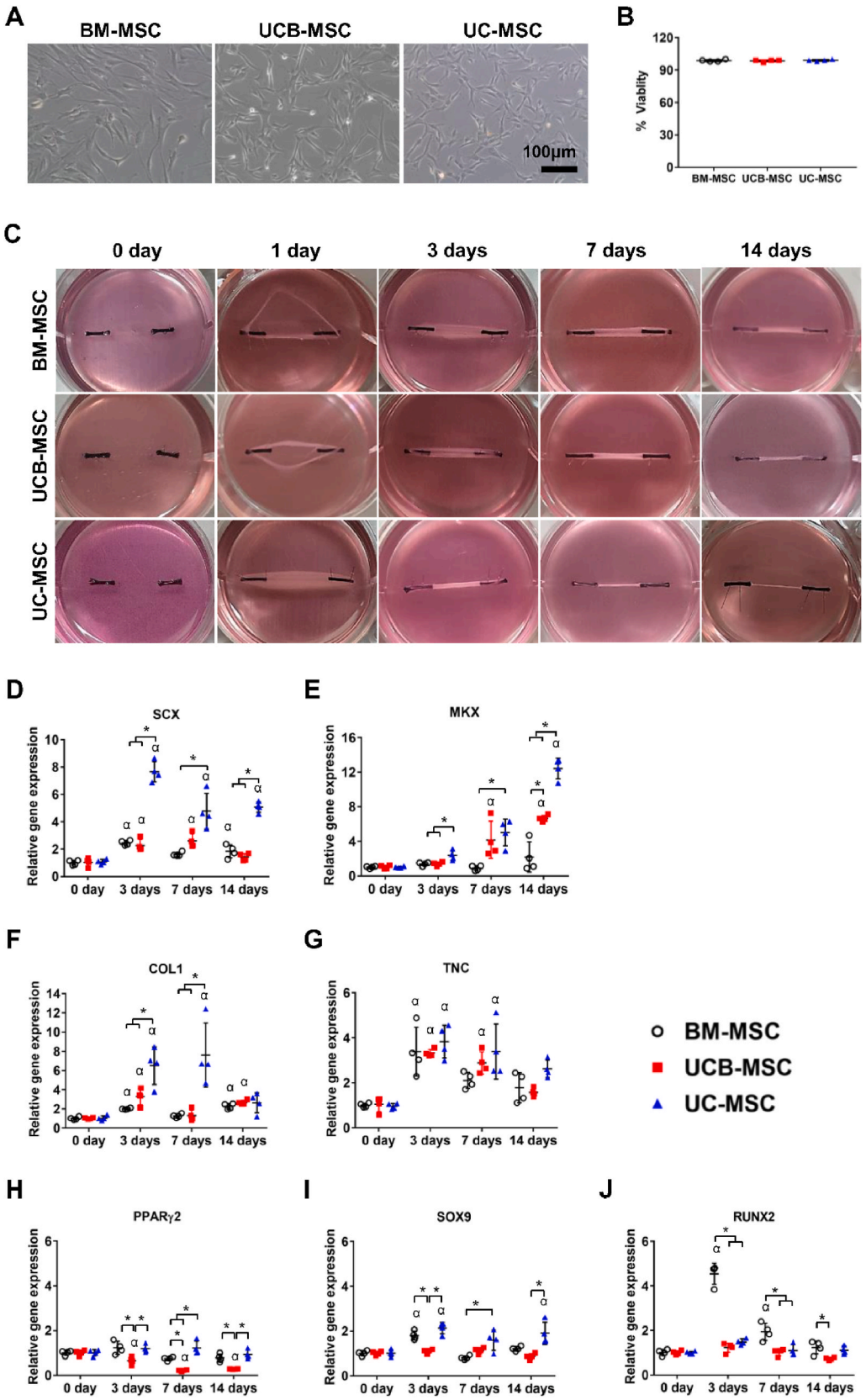

Fig. 1. Characterization of BM-, UCB- and UC-MSC and gene expressions related to tenogenic, adipogenic, chondrogenic and osteogenic differentiations. (A) Fibroblast-like morphology of cells (magnification; X100). (B) Viability evaluated by trypan blue exclusion. (C) Macroscopic appearance in T-3D condition. Gene expression of SCX (D), MKX (E), COL1 (F), TNC (G), PPARγ1 (H), SOX9 (I) and RUNK2 (J). Bar charts represent mean ± standard deviation; statistically significant at $p < 0.050$ (* means significant difference among groups and α means significant difference compared to 0 day). (For interpretation of the references to colour in this figure legend, the reader is referred to the Web version of this article.)

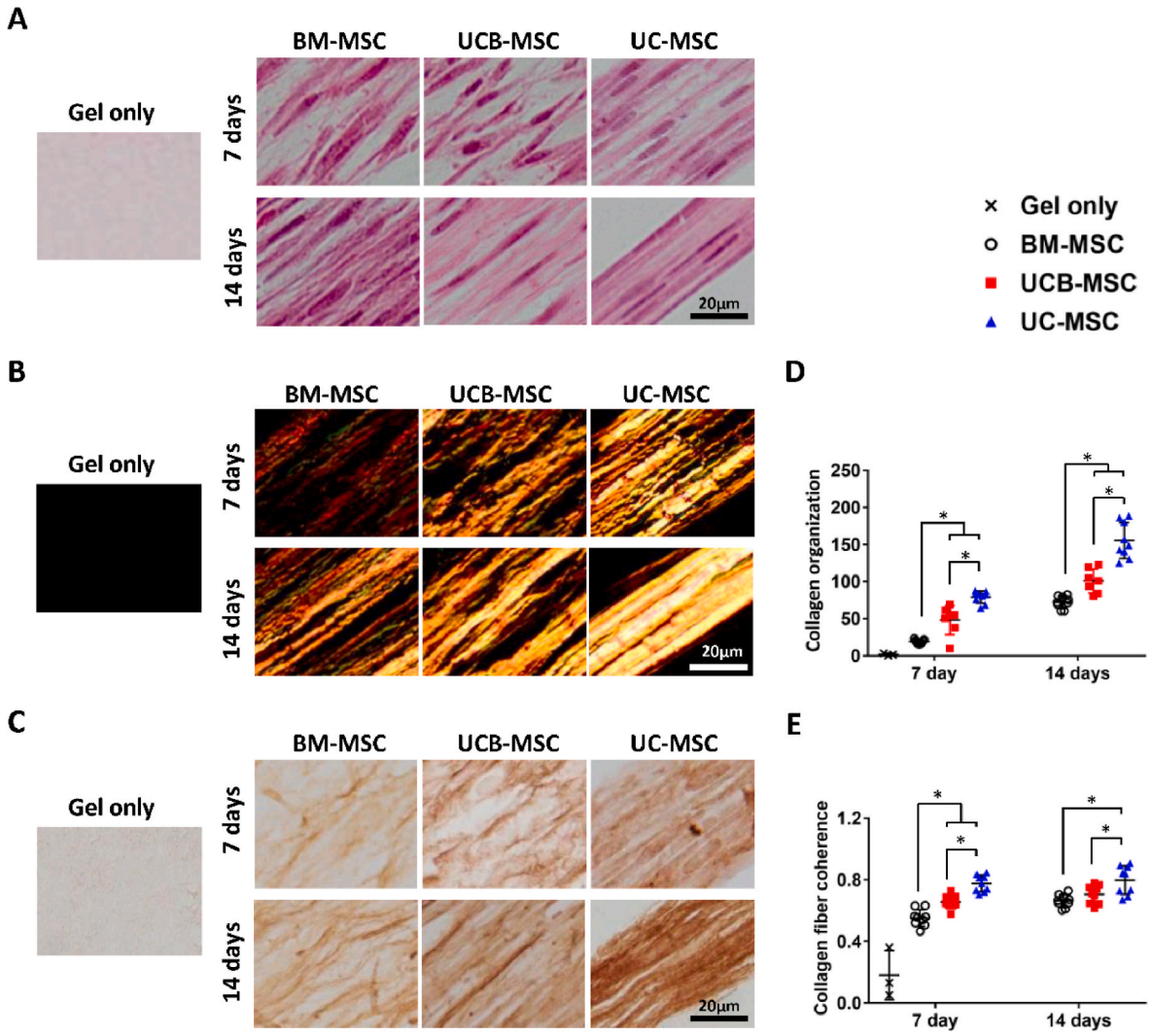

Fig. 2. Histological evaluation of matrix formed by BM-, UCB- and UC-MSC on days 7 and 14. (A) H&E staining of formed matrix. (B) PSR staining of formed matrix. (C) IHC of type I collagen in the matrix (magnification; X1000). (D) Collagen organization in the matrix formed. (E) Collagen fiber coherence in the formed matrix. Bar charts represent mean ± standard deviation; statistically significant at $p < 0.050$.

Saline (Fig. 4E and F).

Overall, these data suggest that UC-MSC have highest ability to enhance tendon regeneration and reduce heterotopic matrix changes after tendon injury compared to other types of MSCs, while BM-MSC could induce heterotopic matrix changes.

3.5. UC-MSC trafficking in FTD of rotator cuff tendon of rats

At four weeks, the mean number of MSCs per area were significantly reduced by 35%, 34% and 31% in BM-MSC, UCB-MSC and UC-MSC groups compared to that at two weeks. However, there was no significant difference among the MSCs groups (Fig. 5). Although the number of MSCs decreased over time, they could remain in the site of tendon for up to 4 weeks and could affect tendon healing directly after injury.

4. Discussion

Depending on the tissue origin, MSCs exhibit different functional characteristics such as tissue regenerative potential [25]. A comparison of these characteristics among MSCs isolated from different tissue sources is necessary to determine the type of MSCs that are more appropriate for a specific disease. Previously, several studies reported that MSCs derived from fetal tissue were more effective than BM-MSC in nerve regeneration [11,26]. Even though UC-MSC exhibit similar morphological, phenotypic and differentiation potential compared to BM-MSC, UC-MSC showed a higher proliferation rate and greater expansion potential than BM-MSC [11,26]. Further, MSCs derived from fetal tissue exhibit greater differentiation into specific cells such as neurons and display higher upregulation of neurotrophic and tissue regeneration-associated genes than MSCs derived from bone marrow [11].

In line with a previous study, we found that UC-MSC exhibited not only a higher upregulation in gene expression related to tenogenic differentiation such as SCX and MKX and tendon matrix-associated genes such as COLI and TNC but also formed well-organized tendon-like matrix compared with that of BM-MSC under T-3D condition. SCX and MKX, key transcription factors for tenogenic differentiation, physically interact with smad3, which transmits TGF-β signaling related to collagen matrix formation and healing. Smad3 modulates gene expression and protein synthesis of COL1 and TNC [6]. Previous studies reported that BM-MSC enhanced by SCX and MKX are more effective in regenerating the structure and tensile strength of tendon compared to naïve BM-MSC after Achilles tendon injury in animal models [10,25]. Thus, UC-MSC with increased expression of these transcription factors exhibit superior tenogenic differentiation and tendon-like matrix formation. In animal models, UC-MSC significantly improved the regeneration of tendon,

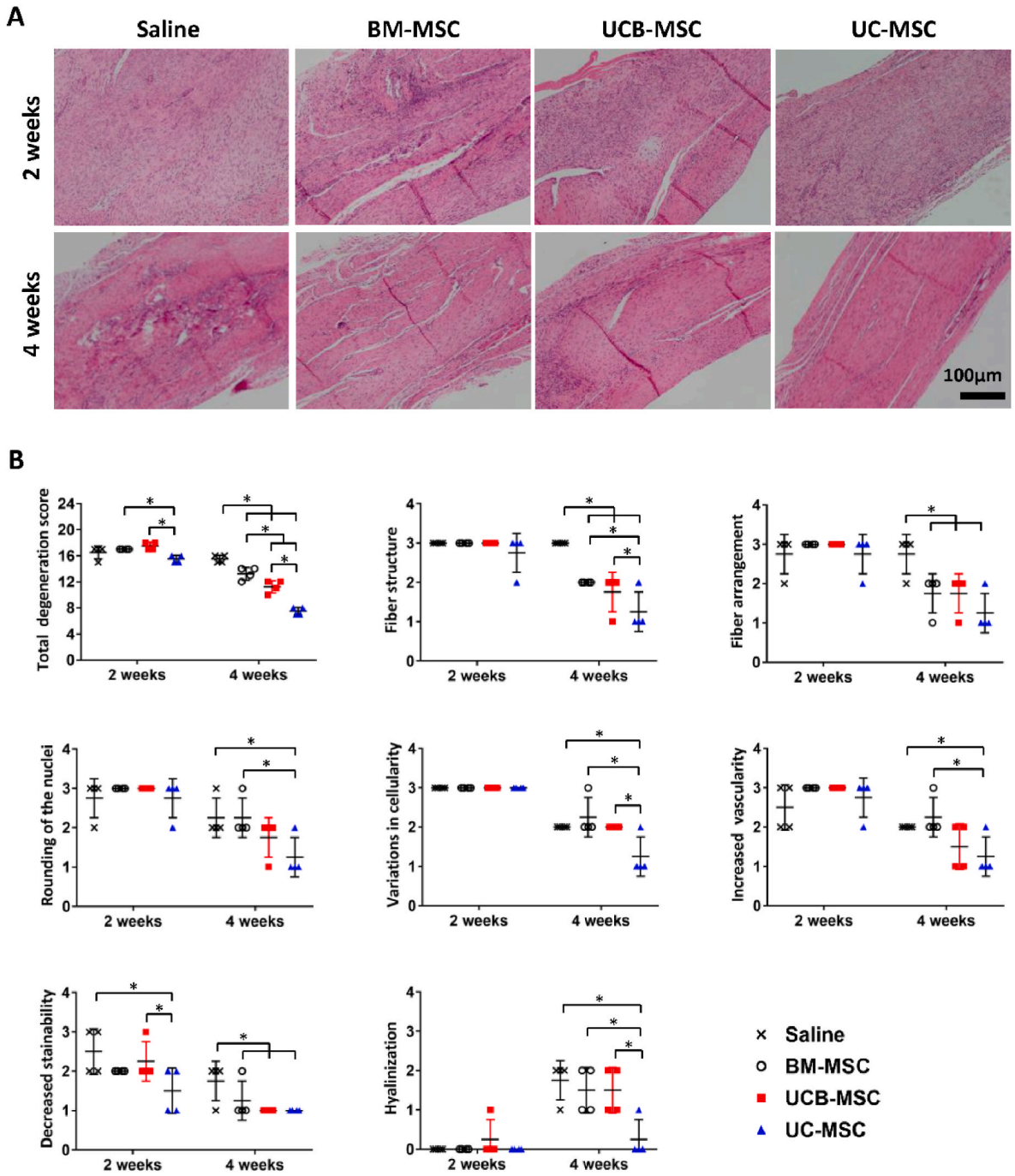

Fig. 3. Histological evaluation of tendon regenerated at two and four weeks after injection with saline, BM-, UCB- and UC-MSC. (A) H&E staining of regenerated tendon (magnification; X200). (B) The total degeneration score and detailed parameters. Bar charts represent mean ± standard deviation; statistically significant at $p < 0.050$.

comprising dense and well-organized type I collagen fibers compared with those of BM-MSC in this study. Furthermore, UC-MSC was more effective than UCB isolated from the fetal tissue.

Additionally, a lot of papers showed that UC-derived MSCs have attractive advantages compared with other origins. They can be easily collected and have a lower risk of infection, a low risk of teratoma and low immunogenicity with a good immunosuppressive ability for clinical use [27–29], . We previously demonstrated that characteristics of UC-MSC are not affected by cryopreservation and exhibit almost similar healing potential for tendon recovery after preparation for an "off-the shelf' usage [14]. These results suggest that UC-MSC represent a good option for tendon regeneration and are recommended for cell therapy of tendon diseases clinically.

Heterotopic matrix formation including GAG-rich area, hyalinization and ossification has been reported in patients with rotator cuff disease [9]. Additionally, chondrocyte-like cells and heterotopic chondro-ossification and erroneous extracellular matrix deposition has been reported in animal models with tendon window defect and collagenase-induced tendinopathy [30,31]. These changes in heterotopic matrix exacerbate the clinical manifestations of tendon disease [32] and induce high rates of re-rupture and increase in recovery time [13]. Eventually, these changes lead to a high frequency of post-operative complications including limitation of movement and shoulder pain [1]. Therefore, suppressing heterotopic matrix change is

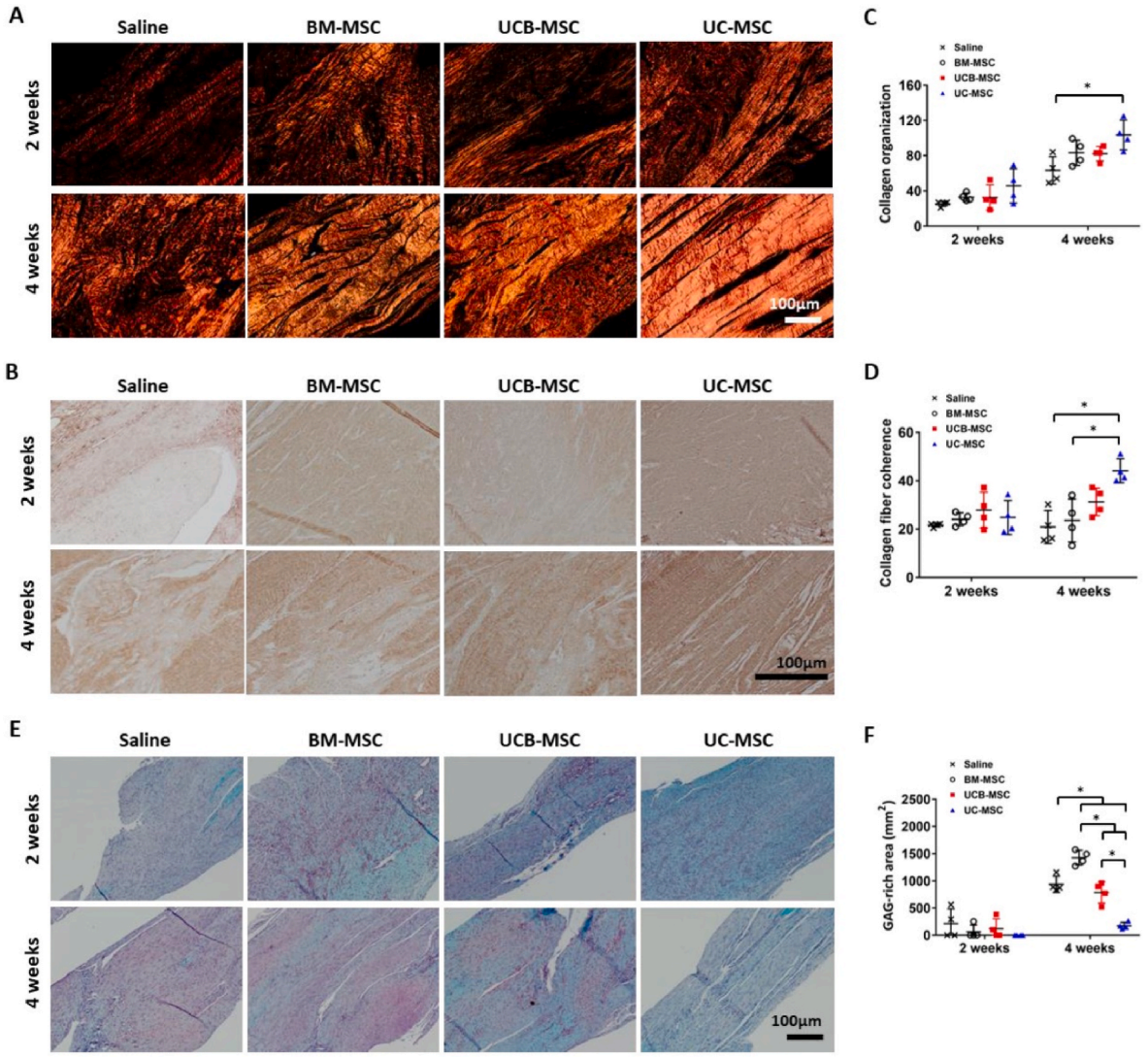

Fig. 4. Quantification of collagen matrix changes and GAG-rich area in regenerated tendon at two and four weeks after injection with Saline, BM-, UCB- and UC-MSC. (A) PSR staining of regenerated tendon. (B) IHC of type I collagen in the regenerated tendon. (C) Collagen organization in the regenerated tendon. (D) Collagen fiber coherence in the regenerated tendon. (E) Saf-O staining of regenerated tendon (magnification; X200). (F) GAG-rich area of regenerated tendon. Bar charts represent mean ± standard deviation; statistically significant at $p < 0.050$.

fundamentally important for the treatment of tendon disease. However, the use of BM-MSC induces heterotopic ossification up to 55% of cases involving tendon defects and in tendinopathy models [2,10]. In line with a previous study of BM-MSC, the regenerated tendon matrix had low-density and disorganized collagen fibers compared with other MSCs and even larger GAG-rich area than that of Saline group because BM-MSC differentiate into osteocyte-like cells due to the tissue origin [26,30]. BM-MSC exhibited high gene expressions related to osteogenesis differentiation, including RUNX2 and a relatively low gene expression related to tenogenic differentiation, involving SCX, MKX and COL1, even in tenogenic differentiation conditions. These results suggest that BM-MSC may facilitate the study of cartilage and bone regeneration, but the differentiation of BM-MSC into unexpected cells and formation of heterotopic matrix such as cartilage or bone within tendon during tendon regeneration, is a concern. However, UC-MSC suppressed heterotopic cartilage-related GAG formation and did not induce any heterotopic ossification. Although the mechanism of inhibition of heterotopic cartilage or bone formation by UC-MSC remains unknown, these results demonstrated that application of UC-MSC is a safer option than BM-MSC in tendon regeneration.

In this study, we observed that three different types of MSCs exhibited upregulated gene expression related to tenogenic differentiation and formed tendon-like matrix in T-3D conditions. Further, they improved the macroscopic appearance and structure of regenerated tendon of FTD until four weeks after MSC injection in a rat model. However, most of the transplanted human MSCs disappeared at the regenerated tendon over time in cell trafficking results, because the advantages of MSCs are attributed not only to the direct differentiation of MSCs into tenocytes but also the paracrine mechanism, which secretes cytokines and growth factors. The secreted factors recruit, proliferate, and differentiate tendon stem/progenitor cells and enhance tendon matrix formation [14,33]. Furthermore, the local inflammatory environment at the injured site is controlled by MSCs by regulating the function of inflammatory cells such as macrophage recruitment, proliferation and polarization to alternatively activated macrophages [3,12]. Additionally, previous studies reported that MSCs derived from the birth tissue are less immunogenic with a lower neutrophil infiltration and more immunosuppressive capacities with effects on the regulatory T cells compared with those of MSCs derived from the adult tissue [6]. Therefore, even though injected UC-MSC decreased eventually, the controlled local environment by UC-MSC has a healing effect on the defective tendon. UC-MSC are safer and more effective than BM-MSC.

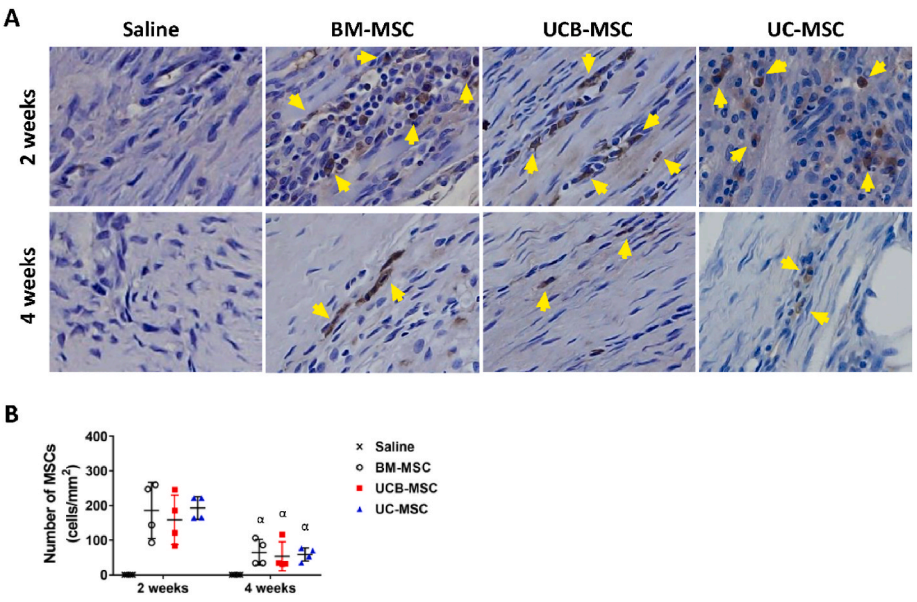

Fig. 5. Cell trafficking of MSCs within the regenerated tendon and quantification of the MSCs at two and four weeks after injection. (A) Mitochondrial staining (IHC) within the tendon (yellow arrows indicate DAB-stained MSCs) (magnification; X400). (B): The number of MSCs per area. Bar charts represent mean ± standard deviation; statistically significant at $p < 0.050$ (α means significant difference between two and four weeks). (For interpretation of the references to colour in this figure legend, the reader is referred to the Web version of this article.)

The study limitations are as follows. First, we used three types of MSCs at different passages; BM-MSC and UCB-MSC were used at passage 5, while UC-MSC was used at passage 10. Senescence of BM-MSC and UCB-MSC are earlier than that of UC-MSC [4]. Thus, we used BM- and UCB-MSC at relatively early passage to avoid aging of MSCs. However, UC-MSC in this study showed greater efficacy than other MSCs in overcoming the disadvantage associated with late passage. Second, we only investigated tendon regeneration briefly after injecting MSCs, which is relatively early to determine the sustained efficacy of MSCs.

5. Conclusion

UC-MSC are superior to other types of MSCs in differentiating into tendon-like lineages and forming a tendon-like matrix in T-3D conditions. Also, UC-MSC improves the regeneration of FTD in histological properties compared to BM- and UCB-MSC.

Funding statements

This research was supported by a grant (NRF-2015M3A9E6028412) of the Bio & Medical Technology Development Program, a grant (NRF-2017R1A2B2010995) of the Basic Science Research Program of the National Research Foundation of Korea and a grant (HI20C0386) of the Korea Health Industry Development Institute (KHIDI).

Declaration of competing interest

The authors declare the following financial interests/personal relationships which may be considered as potential competing interests: C. H.J. owns shares of AcesoStem Biostrategies Inc. The other authors indicated no potential conflicts of interest.

Appendix A. Supplementary data

Supplementary data to this article can be found online at https://doi.org/10.1016/j.bbrep.2023.101486.

References

[1] M. Schneider, P. Angele, T.A.H. Jarvinen, D. Docheva, Rescue plan for Achilles: therapeutics steering the fate and functions of stem cells in tendon wound healing, Adv. Drug Deliv. Rev. 129 (2018) 352–375.
[2] D. Van der Windt, B.W. Koes, A. Boeke, W. Devillé, B.A. De Jong, L.M. Bouter, Shoulder disorders in general practice: prognostic indicators of outcome, Br. J. Gen. Pract. 46 (1996) 519–523.
[3] S.T. Bianco, H.L. Moser, L.M. Galatz, A.H. Huang, Biologics and stem cell-based therapies for rotator cuff repair, Ann. N. Y. Acad. Sci. 1442 (2018) 35–47.
[4] X.N. Liu, C.J. Yang, J.E. Kim, Z.W. Du, M. Ren, W. Zhang, H.Y. Zhao, K.O. Kim, K. C. Noh, Enhanced tendon-to-bone healing of chronic rotator cuff tears by bone marrow aspirate concentrate in a rabbit model, Clin. Orthop. Surg. 10 (2018) 99–110.
[5] M.P. De Miguel, S. Fuentes-Julian, A. Blazquez-Martinez, C.Y. Pascual, M.A. Aller, J. Arias, F. Arnalich-Montiel, Immunosuppressive properties of mesenchymal stem cells: advances and applications, Curr. Mol. Med. 12 (2012) 574–591.
[6] C. Laroye, A. Boufenzer, L. Jolly, L. Cunat, C. Alauzet, J.L. Merlin, C. Yguel, D. Bensoussan, L. Reppel, S. Gibot, Bone marrow vs Wharton's jelly mesenchymal stem cells in experimental sepsis: a comparative study, Stem Cell Res. Ther. 10 (2019) 192.
[7] L.N. Zhou, J.C. Wang, P.L.M. Zilundu, Y.Q. Wang, W.P. Guo, S.X. Zhang, H. Luo, J. H. Zhou, R.D. Deng, D.F. Chen, A comparison of the use of adipose-derived and bone marrow-derived stem cells for peripheral nerve regeneration in vitro and in vivo, Stem Cell Res. Ther. 11 (2020).
[8] H. Uthoff, A. Spenner, W. Reckelkamm, B. Ahrens, G. Wolk, R. Hackler, F. Hardung, J. Schaefer, A. Scheffold, H. Renz, U. Herz, Critical role of preconceptional immunization for protective and nonpathological specific immunity in murine neonates, J. Immunol. 171 (2003) 3485–3492.
[9] D.L. Troyer, M.L. Weiss, Concise review: wharton's jelly-derived cells are a primitive stromal cell population, Stem Cell. 26 (2008) 591–599.
[10] C.F. Hsieh, P. Alberton, E. Loffredo-Verde, E. Volkmer, M. Pietschmann, P. Muller, M. Schieker, D. Docheva, Scaffold-free Scleraxis-programmed tendon progenitors aid in significantly enhanced repair of full-size Achilles tendon rupture, Nanomedicine (Lond) 11 (2016) 1153–1167.
[11] D.R. Kwon, G.Y. Park, S.C. Lee, Treatment of full-thickness rotator cuff tendon tear using umbilical cord blood-derived mesenchymal stem cells and polydeoxyribonucleotides in a rabbit model, Stem Cell. Int. 2018 (2018), 7146384.
[12] C. Brown, C. Mckee, S. Bakshi, K. Walker, E. Hakman, S. Halassy, D. Svinarich, R. Dodds, C.K. Govind, G.R. Chaudhry, Mesenchymal stem cells: cell therapy and regeneration potential, J. Tissue Eng. Regen. Med. 13 (2019) 1738–1755.
[13] N. Beeravolu, I. Khan, C. Mckee, S. Dinda, B. Thibodeau, G. Wilson, M. Perez-Cruet, R. Bahado-Singh, G.R. Chaudhry, Isolation and comparative analysis of potential stem/progenitor cells from different regions of human umbilical cord, Stem Cell Res. 16 (2016) 696–711.
[14] J.-H. Yea, J.-K. Park, I.J. Kim, G. Sym, T.-S. Bae, C.H. Jo, Regeneration of a full-thickness defect of rotator cuff tendon with freshly thawed umbilical cord-derived mesenchymal stem cells in a rat model, Stem Cell Res. Ther. 11 (2020) 1–13.
[15] J.H. Kim, C.H. Jo, H.R. Kim, Y.I. Hwang, Comparison of immunological characteristics of mesenchymal stem cells from the periodontal ligament, umbilical cord, and adipose tissue, Stem Cell. Int. 2018 (2018), 8429042.
[16] A.Y. Lee, K.H. Jang, C.H. Jo, Minimal cube explant provides optimal isolation condition of mesenchymal stem cells from umbilical cord, Tissue Eng. Regen. Med. 19 (2022) 793–807.
[17] C.H. Jo, O.S. Kim, E.Y. Park, B.J. Kim, J.H. Lee, S.B. Kang, J.H. Lee, H.S. Han, S. H. Rhee, K.S. Yoon, Fetal mesenchymal stem cells derived from human umbilical cord sustain primitive characteristics during extensive expansion, Cell Tissue Res. 334 (2008) 423–433.

[18] C. Lebled, L.M. Grover, J.Z. Paxton, Combined decellularisation and dehydration improves the mechanical properties of tissue-engineered sinews, J. Tissue Eng. 5 (2014), 2041731414536720.
[19] J.-H. Yea, S. Shin, K.S. Yoon, C.H. Jo, Effects of corticosteroids and platelet-rich plasma on synoviocytes in IL-1ß-induced inflammatory condition, Connect. Tissue Res. (2021) 1–11.
[20] C.H. Jo, W.H. Shin, J.W. Park, J.S. Shin, J.E. Kim, Degree of tendon degeneration and stage of rotator cuff disease, Knee Surg. Sports Traumatol. Arthrosc. 25 (2017) 2100–2108.
[21] T.M. Kraus, F.B. Imhoff, J. Reinert, G. Wexel, A. Wolf, D. Hirsch, A. Hofmann, U. Stockle, S. Buchmann, T. Tischer, A.B. Imhoff, S. Milz, M. Anton, S. Vogt, Stem cells and bFGF in tendon healing: effects of lentiviral gene transfer and long-term follow-up in a rat Achilles tendon defect model, BMC Muscoskel. Disord. 17 (2016) 1–7.
[22] J.H. Yea, I. Kim, G. Sym, J.K. Park, A.Y. Lee, B.C. Cho, T.S. Bae, B.J. Kim, C.H. Jo, Regeneration of a full-thickness defect in rotator cuff tendon with umbilical cord-derived mesenchymal stem cells in a rat model, PLoS One 15 (2020), e0235239.
[23] E.S. Kang, K.Y. Ha, Y.H. Kim, Fate of transplanted bone marrow derived mesenchymal stem cells following spinal cord injury in rats by transplantation routes, J. Kor. Med. Sci. 27 (2012) 586–593.
[24] J.-H. Yea, T.S. Bae, B.J. Kim, Y.W. Cho, C.H. Jo, Regeneration of the rotator cuff tendon-to-bone interface using umbilical cord-derived mesenchymal stem cells and gradient extracellular matrix scaffolds from adipose tissue in a rat model, Acta Biomater. (2020).
[25] S. Balasubramanian, P. Venugopal, S. Sundarraj, Z. Zakaria, A.S. Majumdar, M. Ta, Comparison of chemokine and receptor gene expression between Wharton's jelly and bone marrow-derived mesenchymal stromal cells, Cytotherapy 14 (2012) 26–33.
[26] J. Hua, J. Gong, H. Meng, B. Xu, L. Yao, M. Qian, Z. He, S. Zou, B. Zhou, Z. Song, Comparison of different methods for the isolation of mesenchymal stem cells from umbilical cord matrix: proliferation and multilineage differentiation as compared to mesenchymal stem cells from umbilical cord blood and bone marrow, Cell Biol. Int. 38 (2014) 198–210.
[27] S.J. Prasanna, D. Gopalakrishnan, S.R. Shankar, A.B. Vasandan, Pro-inflammatory cytokines, IFNγ and TNFα, influence immune properties of human bone marrow and Wharton jelly mesenchymal stem cells differentially, PLoS One 5 (2010), e9016.
[28] D. Polchert, J. Sobinsky, G. Douglas, M. Kidd, A. Moadsiri, E. Reina, K. Genrich, S. Mehrotra, S. Setty, B. Smith, IFN-γ activation of mesenchymal stem cells for treatment and prevention of graft versus host disease, Eur. J. Immunol. 38 (2008) 1745–1755.
[29] T. Nagamura-Inoue, H. He, Umbilical cord-derived mesenchymal stem cells: their advantages and potential clinical utility, World J. Stem Cell. 6 (2014) 195.
[30] K. Drela, W. Lech, A. Figiel-Dabrowska, M. Zychowicz, M. Mikula, A. Sarnowska, K. Domanska-Janik, Enhanced neuro-therapeutic potential of Wharton's Jelly-derived mesenchymal stem cells in comparison with bone marrow mesenchymal stem cells culture, Cytotherapy 18 (2016) 497–509.
[31] E. Berthet, C. Chen, K. Butcher, R.A. Schneider, T. Alliston, M. Amirtharajah, Smad3 binds Scleraxis and Mohawk and regulates tendon matrix organization, J. Orthop. Res. 31 (2013) 1475–1483.
[32] H. Liu, C. Zhang, S. Zhu, P. Lu, T. Zhu, X. Gong, Z. Zhang, J. Hu, Z. Yin, B.C. Heng, Mohawk promotes the tenogenesis of mesenchymal stem cells through activation of the TGFβ signaling pathway, Stem Cell. 33 (2015) 443–455.
[33] R. El Omar, J. Beroud, J.F. Stoltz, P. Menu, E. Velot, V. Decot, Umbilical cord mesenchymal stem cells: the new gold standard for mesenchymal stem cell-based therapies? Tissue Eng. B Rev. 20 (2014) 523–544.